



Since January 2020 Elsevier has created a COVID-19 resource centre with free information in English and Mandarin on the novel coronavirus COVID-19. The COVID-19 resource centre is hosted on Elsevier Connect, the company's public news and information website.

Elsevier hereby grants permission to make all its COVID-19-related research that is available on the COVID-19 resource centre - including this research content - immediately available in PubMed Central and other publicly funded repositories, such as the WHO COVID database with rights for unrestricted research re-use and analyses in any form or by any means with acknowledgement of the original source. These permissions are granted for free by Elsevier for as long as the COVID-19 resource centre remains active.

equipment and reagents necessary for the preparation of specimens for confocal scanning are available in any well-stocked histology laboratory. Although originally developed to facilitate viral diagnosis by EM, the methods described herein can be applied to the ultrastructural study of any focal pathologic process.

Acknowledgments

The authors are indebted to Dr. Emilie Morpew for critical review of the manuscript and to Dr. Charleen Chu for helpful discussions.

[33] Using Confocal Microscopy to Study Virus Binding and Entry into Cells

By ALAIN VANDERPLASSCHEN and GEOFFREY L. SMITH

Introduction

For decades, the quantitative study of virus binding and entry relied on assays requiring the use of purified virus preparations that were labeled in some way. One approach was to incorporate radioactive tracers into the culture medium during virus growth and then to purify radioactive virus. Other approaches involved labeling the virus after purification by nonradioactive methods such as biotinylation^{1,2} or incorporation of fluorescent label.³ The results generated were relative numbers representing the mean number of virions bound to the cell population⁴ or individual cells.¹ We have developed new approaches to study vaccinia virus (VV) binding and entry based on confocal microscopy. These techniques do not require virus purification or labeling and generate data that reveal the absolute numbers of virus particles that have bound to or have entered into individual cells.

In this article, these techniques are described and then illustrated with some of the results obtained. Although the utility of the techniques reviewed here have been demonstrated with VV, given the resolution of the confocal microscope, these methods should be applicable to any virus larger than

¹ G. Inghirami, M. Nakamura, J. E. Balow, A. L. Notkins, and P. Casali, *J. Virol.* **62**, 2453 (1988).

² P. Borrow and M. B. Oldstone, *J. Virol.* **66**, 7270 (1992).

³ R. W. Doms, R. Blumenthal, and B. Moss, *J. Virol.* **64**, 4884 (1990).

⁴ A. Vanderplasschen, M. Bublot, J. Dubuisson, P.-P. Pastoret, and E. Thiry, *Virology* **196**, 232 (1993).

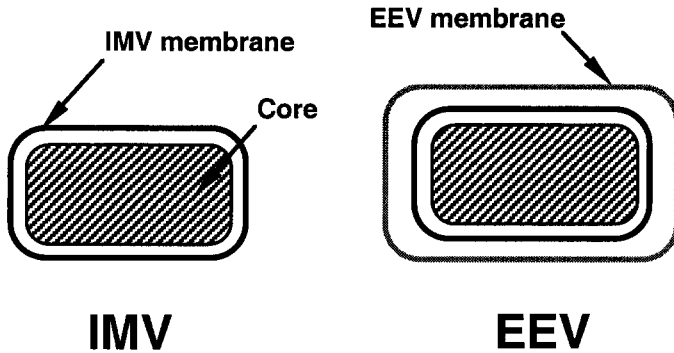


Fig. 1. Schematic representation of IMV and EEV structure.

50 nm. Finally, we will discuss how these techniques have generated data that cannot be obtained with classical binding or entry assays.

Vaccinia virus is the prototype of the poxvirus family (for review, see Moss⁵). These are DNA viruses that replicate in the cell cytoplasm and have genomes between 150 and 300 kbp. The virions are large and complex, and in the case of VV, have dimensions of 250 × 350 nm and contain more than 100 proteins.⁶ The study of VV binding and entry has been complicated by the fact that there are two morphologically distinct infectious virions, termed intracellular mature virus (IMV) and extracellular enveloped virus (EEV).^{7,8} Structurally, IMV consists of a core surrounded by one membrane,^{9,10} whereas EEV consists of an IMV with an additional outer membrane containing proteins, which is absent from IMV (Fig. 1). IMV remains within the cytoplasm until cell lysis and represents the majority of infectious progeny; for instance, with the Western Reserve (WR) strain of virus, IMV represents 99% of infectivity. In contrast, EEV is released actively from infected cells before cell lysis and is the form of the virus that is important for virus dissemination *in vitro* and *in vivo*.^{7,11–13}

Extracellular enveloped virus is formed by the wrapping of IMV with

⁵ B. Moss, in "Virology" (B. N. Fields, D. M. Knipe, P. M. Howley, R. M. Chanock, J. Melnick, T. P. Monath, B. Roizman, and S. E. Straus, eds.), p. 2637. Lippincott-Raven, Philadelphia, 1996.

⁶ K. Essani and S. Dales, *Virology* **95**, 385 (1979).

⁷ G. Appleyard, A. J. Hapel, and E. A. Boulter, *J. Gen. Virol.* **13**, 9 (1971).

⁸ Y. Ichihashi, S. Matsumoto, and S. Dales, *Virology* **46**, 507 (1971).

⁹ S. Dales and E. H. Mosbach, *Virology* **35**, 564 (1968).

¹⁰ M. Hollinshead, A. Vanderplassen, G. L. Smith, and D. J. Vaux, *J. Virol.*, in press (1999).

¹¹ E. A. Boulter and G. Appleyard, *Prog. Med. Virol.* **16**, 86 (1973).

¹² L. G. Payne and K. Kristensson, *J. Gen. Virol.* **66**, 643 (1985).

¹³ L. G. Payne, *J. Gen. Virol.* **50**, 89 (1980).

two membranes derived from the trans-Golgi network or early tubular endosomes forming an intracellular enveloped particle (IEV) that has three membranes. This particle moves to the cell surface where a fusion event between the plasma membrane and the outer membrane of IEV forms a virus with two membranes. This particle may remain attached to the cell surface as cell-associated enveloped virus (CEV) or be released from the cell as EEV. The proportion of enveloped virus that is either retained on the cell surface or released into the medium varies with different strains of virus. At least 12 proteins that are absent from IMV are associated with the outer envelope of EEV.¹⁴⁻¹⁶ Six VV genes are known to encode these proteins (for review, see Smith and Vanderplasschen¹⁷) and, in addition, several cellular proteins are present in the EEV envelope.¹⁶ These proteins endow EEV with different biological and immunological properties.^{7,11,16,18}

The presence of these two infectious forms of virus complicates studies investigating the binding of virions to cells or entry into cells. In order to obtain data relating to only one form of the virus, it is necessary to either purify the different viruses from each other and to study each in isolation or devise a method to study both forms simultaneously within a mixed preparation and to distinguish one from the other. The extra membrane of EEV gives the virus different physical properties such that it may be separated from IMV by sedimentation through CsCl density gradients.¹⁴ In these gradients, IMV and EEV sediment at 1.27 and 1.23 g/ml, respectively.¹⁴ However, the EEV outer membrane is a loose and extremely fragile structure¹⁹ that is damaged by virus purification,^{17,20-22} and once it is ruptured, the particle retains full infectivity as an IMV.^{23,24} Consequently, the mechanism of binding and penetration of intact EEV may be different from that of damaged EEV having IMV proteins exposed on its surface.^{17,20-22} Therefore, binding and penetration studies should not be performed using purified EEV. To overcome this problem, we developed

¹⁴ L. G. Payne, *J. Virol.* **27**, 28 (1978).

¹⁵ L. G. Payne, *J. Virol.* **31**, 147 (1979).

¹⁶ A. Vanderplasschen, E. Mathew, M. Hollinshead, R. B. Sim, and G. L. Smith, *Proc. Natl. Acad. Sci. U.S.A.* **95**, 7544 (1998).

¹⁷ G. L. Smith and A. Vanderplasschen, in "Coronaviruses and Arteriviruses" (L. Enjuanes, S. G. Siddell, and W. Spaan, eds.), p. 395. Plenum Press, London, 1998.

¹⁸ G. S. Turner and E. J. Squires, *J. Gen. Virol.* **13**, 19 (1971).

¹⁹ N. Roos, M. Cyrklaff, S. Cudmore, R. Blasco, J. Krijnse-Locker, and G. Griffiths, *EMBO J.* **15**, 2343 (1996).

²⁰ A. Vanderplasschen and G. L. Smith, *J. Virol.* **71**, 4032 (1997).

²¹ A. Vanderplasschen, M. Hollinshead, and G. L. Smith, *J. Gen. Virol.* **78**, 2041 (1997).

²² Y. Ichihashi, *Virology* **217**, 478 (1996).

²³ A. A. G. McIntosh and G. L. Smith, *J. Virol.* **70**, 272 (1996).

²⁴ E. J. Wolffe, E. Katz, A. Weisberg, and B. Moss, *J. Virol.* **71**, 3904 (1997).

binding and entry assays that allow the use of fresh supernatants of infected cells as the source of EEV. These assays are based on confocal microscopy and the use of monoclonal antibodies that are specific to each form of the virus.

Methods

Cells and Virus

RK₁₃ cells are grown in minimum essential medium (MEM) (GIBCO) containing 10% heat-inactivated fetal bovine serum (HFBS). HeLa cells are grown as suspension cultures as described elsewhere.²⁵ The IHD-J VV strain is used throughout. Fresh EEV and purified IMV are prepared as described previously.²⁰ Briefly, for fresh EEV, cells are infected at 1 plaque-forming unit (pfu)/cell, and the culture supernatant is harvested 24 hr postinfection (hpi) and clarified by centrifugation at 2000g. After appropriate dilution, any contaminating IMV infectivity is neutralized by the addition of monoclonal antibody (MAb) 5B4/2F2 (final dilution of 1/2560) against the 14-kDa fusion protein (A27L gene product) of IMV.²⁶ In the conditions used in this study, MAb 5B4/2F2 neutralizes >93% of purified IMV. A fresh EEV preparation is produced for each experiment and, except where stated otherwise, MAb 5B4/2F2 is added to these EEV samples.

MAbs and Rabbit Antiserum

The culture supernatant from murine hybridoma secreting the IgM MAb B2 was kindly provided by Dr. W. Chang.²⁷ MAb B2 bound to the cell surface is shown to prevent IMV binding, but its effect on EEV binding or infectivity is unknown. Murine MAb AB1.1 (α -D8L)²⁸ and rat MAb 19C2 (α -B5R)²⁹ are raised against the D8L and B5R surface proteins of IMV and EEV, respectively. A rabbit antiserum, hereafter called anticore (α -core), is raised against VV cores isolated as described.³⁰ This serum recognizes the core proteins encoded by genes A10L, A3L, F18R, L4R, and A4L and was kindly provided by Gareth Griffiths (EMBL, Germany).

²⁵ P. R. Cook and I. A. Brazell, *J. Cell Sci.* **19**, 261 (1975).

²⁶ C. P. Czerny and H. Mahnel, *J. Gen. Virol.* **71**, 2341 (1990).

²⁷ W. Chang, J.-C. Hsiao, C.-S. Chung, and C.-H. Bair, *J. Virol.* **69**, 517 (1995).

²⁸ J. E. Parkinson and G. L. Smith, *Virology* **204**, 376 (1994).

²⁹ M. Schmelz, B. Sodeik, M. Ericsson, E. J. Wolffe, H. Shida, and G. Griffiths, *J. Virol.* **68**, 130 (1994).

³⁰ S. Cudmore, R. Blasco, R. Vincentelli, M. Esteban, B. Sodeik, G. Griffiths, and J. Krijnse Locker, *J. Virol.* **70**, 6909 (1996).

Indirect Immunofluorescent Staining

Samples are fixed in phosphate-buffered saline (PBS) containing 4% paraformaldehyde (PFA) (w/v) for 20 min on ice and 40 min at 20°. Immunofluorescent staining (incubation and washes) of fixed samples is performed in PBS containing 10% HFBS (v/v) (PBSF). When permeabilization is required after fixation, the staining is performed in PBSF containing 0.1% (w/v) saponin (Sigma, Poole, Dorset, UK). The samples are incubated at 37° for 45 min with α -D8L (diluted 1/300), biotinylated α -D8L (diluted 1/100), α -B5R (diluted 1/16), or rabbit α -core serum (diluted 1/1000) as the primary antibody. After three washes, the samples are incubated at 37° for 30 min with fluorescein isothiocyanate (FITC)-conjugated F(ab')₂ goat antimouse IgG (FITC-GAM) (8 μ g/ml) (Sigma), rhodamine-conjugated streptavidin (Rd-Strep) (3.3 μ g/ml) (Serotec, Kidlington, Oxon, UK), FITC (10 μ g/ml) (Serotec), R-phycoerythrin (PE) (10 μ g/ml) (Serotec)-conjugated F(ab')₂ rabbit antirat IgG (FITC-RAR, PE-RAR), FITC (6 μ g/ml) (Sigma), or Rd (10 μ g/ml) (ICN, Costa Mesa, CA)-conjugated goat IgG antirabbit IgG (FITC-GARb, Rd-GARb) as secondary conjugates. Samples are mounted in Mowiol mounting medium as described.²¹

Capping of MAb B2 Reactive Epitope

Capping of MAb B2 reactive epitope is induced in HeLa cells grown in suspension as described.²⁰ Undiluted hybridoma supernatant containing MAb B2 is added to HeLa cells for 1 hr on ice, and unbound antibody is removed by washing the cells with PBSF. Rabbit antimouse IgM is added for 30 min on ice. After further washing with PBSF, the cells are warmed to 37° for 10 min to permit capping and then recooled on ice.

Staining of Cell Plasma Membrane

The plasma membrane is stained with FITC-labeled wheat germ agglutinin (FITC-WGA) (5 μ g/ml) (Vector Laboratories Ltd., Peterborough, UK) for 20 min on ice as described previously.³¹ After extensive washing with PBSF and a final wash with PBS, the cells are fixed in PBS containing 4% paraformaldehyde (PFA) (w/v) for 20 min on ice and for 40 min at 20°.

Staining of Lysosomes

Lysosomes are visualized by labeling living cells with lysine PFA-fixable Rd-conjugated dextran (Rd-dextran) (final concentration 100 μ g/ml, Mo-

³¹ A. Vanderplasschen, M. Hollinshead, and G. L. Smith, *J. Gen. Virol.* **79**, 877 (1998).

lecular Probes, Eugene, OR) as described.³¹ After extensive washing with PBSF, the cells are incubated with normal culture medium for 6 hr at 37°.

Confocal Microscopy Analysis

Cells are analyzed with a Bio-Rad (Richmond, CA) MRC 1000 confocal microscope (running under Comos software) using appropriate filters, a full dynamic range of gray scale, and Kalman filtration. Optical sections perpendicular to the *Z* axis are performed throughout the sample. Except where stated otherwise, the confocal pictures are reconstructed by the projection of sections so that the total number of virions bound on the cell surface (for binding assay) or the total number of cores inside the cell (for entry assay) could be determined by examination of the reconstructed picture.

Statistical Analysis

Student's *t* test is used to test for the significance of the results ($P < 0.05$).

Results

Our first approach to study IMV and EEV binding to cells was to use IMV and EEV that had been purified from infected cells (IMV) or the culture supernatant (EEV) and then detect these particles on the cell surface by fluorescent microscopy. IMV was purified using sucrose density gradient centrifugation as described by Joklik.³² EEV was purified from the culture supernatant by first removing detached cells and large cell debris by low-speed centrifugation and then pelleting the virus by ultracentrifugation. The pelleted virus was then resuspended by vortexing and sonication and was purified on CsCl or sucrose density gradients. While CsCl gradients in particular give good separation of IMV and EEV, it was discovered that the majority of EEV particles purified from density gradients had a damaged outer envelope. This was shown by the neutralization of the majority of infectivity in these preparations by a monoclonal antibody specific for IMV (methods). The ability of an IMV-specific antibody to neutralize "EEV" indicated that the integrity of the EEV outer envelope was broken and IMV antigens were exposed, and consequently it would be unknown if the virions were binding to cells via antigens present on the IMV or EEV

³² W. K. Joklik, *Virology* **18**, 9 (1962).

surface. Thus data obtained with such preparations would be uninterpretable.

Attempts to purify EEV by other less vigorous methods also failed to retain the integrity of the EEV envelope and even pelleting the virus and resuspension was found to damage a significant proportion of the virions. Therefore this approach was abandoned and instead we devised a method that used a preparation of virus that contained both IMV and EEV and simultaneously identified and distinguished these particles from each other.

Virus-Binding Assay Using Confocal Microscopy

Vaccinia virus is a very large virus (approximately 250×350 nm) and individual virions had been detected by fluorescent microscopy.³³ Therefore we investigated whether indirect immunofluorescent staining of virions and confocal microscopy could be used to develop a novel virus-binding assay. The idea was to quantify the number of individual virions bound on the cell surface at 4° (a temperature that prevents virus entry). The infectivity of fresh culture supernatant was found to contain mostly EEV, but was contaminated with a significant proportion (15–25%) of IMV, and therefore its use for binding studies required an assay that permitted the differentiation of IMV and EEV. With that goal in mind, we used a double immunofluorescent staining with MAb AB 1.1 and MAb 19C2 against the D8L and B5R gene products, respectively, on fixed and permeabilized samples (Fig. 2). D8L encodes a 32-kDa protein present on the IMV surface²⁸ and 19C2 detects the EEV-specific 42-kDa glycoprotein B5R.²⁹ Biotinylated MAb AB1.1 and MAb 19C2 were used as primary MAbs and were subsequently revealed by Rd-Strep and FITC-RAR, respectively. Following this staining procedure, EEV virions appeared as double positive (red and green) foci, whereas IMV virions were single (red) fluorescent foci on the cell surface. Each fluorescent focus was shown to represent an isolated particle and not a cluster of virions by measuring the size of the spots. The mean diameter of Rd fluorescent foci was 409.3 nm (SD = 13.1, $n = 20$), which is similar to the dimension of a single vaccinia virion.

The use of confocal microscopy rather than conventional epifluorescent microscopy allowed the determination of the total number of virions bound on the cell surface by examining the single image reconstructed by projection of the horizontal sections performed throughout the sample. To obtain the same data by conventional microscopy would require careful examination of a series of pictures taken at different focal planes throughout the sample.

³³ S. Cudmore, P. Cossart, G. Griffiths, and M. Way, *Nature* **378**, 636 (1995).

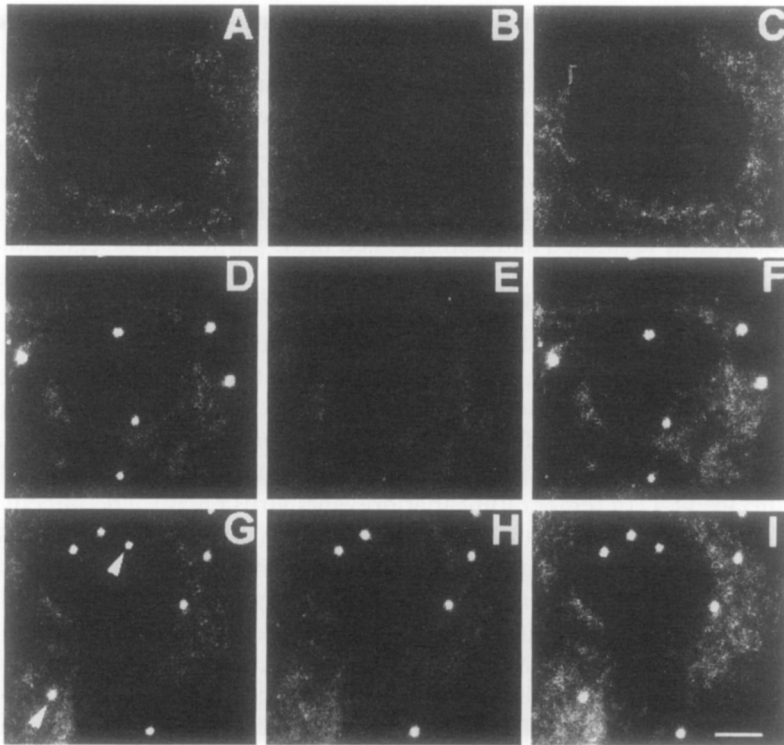


FIG. 2. Detection and identification of IMV and EEV on the cell surface by double immunofluorescent staining and confocal microscopy. RK₁₃ cells were mock infected (A–C) or infected on ice with purified IMV (D–F) or fresh EEV (G–I). The cells were then treated as described in Methods for the simultaneous detection of D8L and B5R gene products by double indirect immunofluorescent staining. Biotinylated MAb AB1.1 and MAb 19C2 were used as primary MABs and were revealed by Rd-Strep and FITC-RAR, respectively. Horizontally, the three panels represent analysis of the same cells. The first (A, D, G) and second (B, E, H) columns of panels represent the analysis for Rd and FITC fluorescent emissions, respectively. The third (C, F, I) column represents the merged Rd and FITC signals. The arrows in (G) identify particles (IMV) that were detected by MAb AB1.1 but not by MAb 19C2. The bar in (I) represents 2 μm . Reproduced from A. Vanderplasschen and G. L. Smith, *J. Virol.* **71**, 4032 (1997), with permission from the American Society for Microbiology.

Particle/Plaque-Forming Unit Ratios for IMV and EEV

The examination of virus preparations by double immunofluorescent staining and microscopy enabled the total number of physical particles to be determined and the proportion of these that were EEV and IMV. The number of infectious particles in a preparation was determined by plaque assay. For purified IMV the great majority (97%, $n = 400$) of physical

particles was IMV and therefore the ratio of total number of particles to the infectious particles (particle/pfu ratio) could be determined. For fresh EEV, the proportion of the infectivity attributable to IMV and EEV was calculated by measuring the infectivity of the virus preparation in the presence or absence of a MAb that neutralized IMV infectivity. These two values enabled the particle/pfu ratios of IMV and EEV in the fresh culture supernatant to be determined. These data showed that EEV had a particle/pfu ratio of 12.7 ± 6.1 ($n = 3$), considerably lower than that of IMV in the same virus preparation (45.0 ± 11.1 , $n = 3$).²⁰ Comparison of the particle/pfu ratios of fresh IMV (45.0 ± 11.1 , $n = 3$) or purified IMV (64.6 ± 16.5 , $n = 3$) showed that the proportion of IMV particles that were infectious decreased during virus purification.²⁰

These data also enabled the determination of the proportion of virus particle bound to cells that gave rise to a plaque. When IMV was added to cells at 10 pfu/cell, 2104 particles bound to 200 cells; therefore each IMV particle that bound gave rise to a plaque $[(2104/200)/10 = 1.052]$. For EEV added to cells at 4.056 pfu/cell, 3984 particles bound to 200 cells. Therefore only approximately 1 in 5 particles gave rise to a plaque $[(3984/200)/4.056 = 4.9]$.²⁰ If the proportion of EEV particles bound to a cell that gave rise to a plaque was five times lower than for IMV particles, how was the greater infectivity (lower particle/pfu ratio) of EEV particles explained? This must reflect differences in the efficiency of either IMV and EEV binding to cells or the subsequent penetration event leading to release of the virus core into the cytoplasm and initiation of the infectious cycle.

IMV and EEV Bind to Different Cellular Receptors

Using the binding assay described in this article we were able to demonstrate unequivocally that IMV and EEV bind to different cellular receptors. Three independent observations allow this conclusion: (1) the efficiency with which IMV and EEV bound to different cell lines was unrelated; (2) cell surface digestion with some enzymes affected IMV and EEV binding differently; and (3) binding of a MAb B2 to cells prevented IMV but not EEV binding.

IMV and EEV Bound to Different Cell Lines with Varying Efficiency

If IMV and EEV bound to an identical receptor, variation in expression of this receptor between different cell lines should affect IMV and EEV binding to the same extent. However, if IMV and EEV bound to separate receptors, the efficiency of IMV and EEV binding might fluctuate independently between different cell lines, reflecting differing levels of expression of the different receptors. Three cells that are used commonly to grow VV

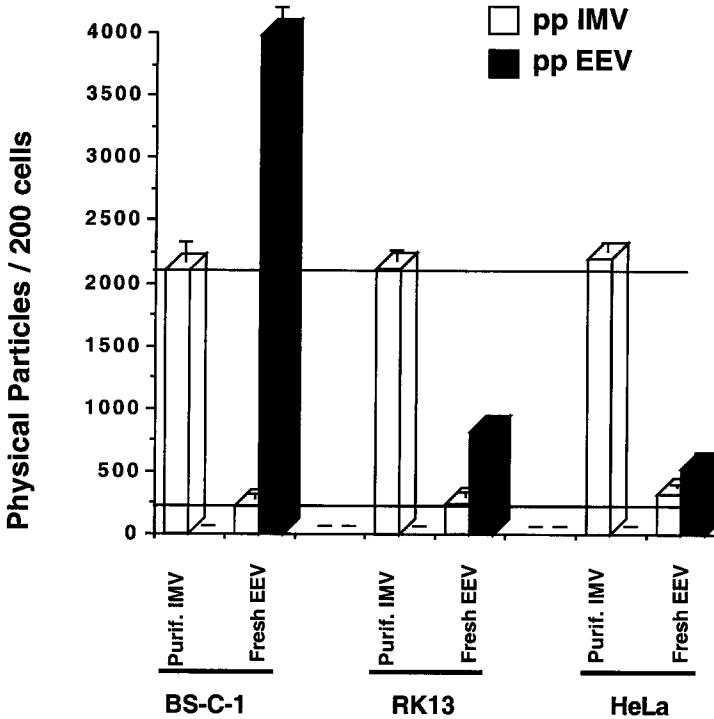


FIG. 3. IMV and EEV binding onto different cell lines. Adherent cells were grown in a 1-well culture chamber slide (Nunc, Life Technologies Ltd., Uxbridge, UK). For HeLa cells, the binding assay was performed in suspension (10^6 cells/ml). Cells were infected on ice for 1 hr (0.5 ml per 1-well chamber slide) with either purified IMV (10 pfu/cell) or fresh EEV (5.2 pfu/cell, 78% of the pfu being resistant to neutralization by MAb 5B4/2F2) diluted in PBS plus 2% FBS. After washing, the cells were treated as described in the text to reveal IMV and EEV virions by double immunofluorescent staining. Numbers of IMV and EEV virions bound on the surface of 200 cells were then determined by confocal microscopy. Data presented are the average \pm SD for triplicate measurements.

were selected for study: human (HeLa) cells in suspension culture, rabbit kidney (RK)₁₃ cells, and African green monkey kidney (BS-C-1) cells. Two different virus preparations were added to these cells: either IMV purified from the cytoplasm of infected cells or fresh EEV from the culture supernatant. In the latter case, the presence of some contaminating IMV enabled the binding of both forms of virus to be analyzed simultaneously and provided a perfect internal control for each form of virus (Fig. 3).

The number of IMV particles bound to the surface of 200 cells was similar for the three cell lines tested. Both sources of IMV (purified IMV and fresh EEV) led to this observation. In contrast, the efficiency of EEV

binding varied between cell lines. For example, 4.9 times more EEV was detected on BS-C-1 cells than on RK₁₃ cells.

The number of plaques formed by IMV or EEV on BS-C-1 and RK₁₃ cells was also investigated. As for the binding assay, the number of plaques formed by IMV was equivalent on both cell types. Whereas fresh EEV, from which contaminating IMV was removed by the addition of IMV-neutralizing antibody, formed fivefold more plaques on BS-C-1 than RK₁₃ cells.²⁰

Cell Surface Digestion with Some Enzymes Affects IMV and EEV Binding Differently

If IMV and EEV bind to separate cellular receptors and if these receptors have different biochemical composition, cell surface treatment with some enzymes might affect the binding of IMV and EEV differently. RK₁₃ cells were digested with trypsin, pronase, or neuraminidase or were mock treated as described previously.²⁰ Purified IMV or fresh EEV (without addition of IMV neutralizing antibody) was then added to these cells and the number of virions bound to the cell was determined (Fig. 4). Trypsin and neuraminidase treatment increased the number of IMV particles bound to cells slightly, whereas pronase treatment reduced IMV binding dramatically. This was true for purified IMV and for IMV present in fresh EEV. These enzymes had quite different effects on EEV binding: trypsin and pronase increased EEV binding approximately two- or threefold, respectively, whereas neuraminidase produced only a small increase. The most spectacular difference between IMV and EEV was observed with pronase, which reduced IMV binding drastically, while enhancing EEV binding. These data were consistent with the proposal that IMV and EEV bind to different cellular receptors.

MAB B2 Bound on the Cell Surface Does Not Affect EEV Binding

Chang *et al.*²⁷ showed that a mouse IgM MAb (MAb B2) bound to a trypsin-sensitive epitope on the cell surface and, when bound, inhibited the binding and consequently infectivity of IMV. This suggested that MAb B2 recognized an IMV receptor. If IMV and EEV bind to an identical receptor, MAb B2 would be expected to affect EEV binding and infectivity to the same extent as IMV. This was addressed using the binding assay described earlier.²⁰ The results demonstrated that when MAb B2 was bound on the cell surface, EEV binding was not inhibited. Moreover, if the MAb B2 reactive antigen was induced to aggregate (capping) by cross-linking with a secondary antibody and warming to 37°, the binding of EEV was still unaffected.²⁰ These results suggest that the MAb B2 reactive receptor is a receptor for IMV but not EEV binding. An alternative, but less likely,

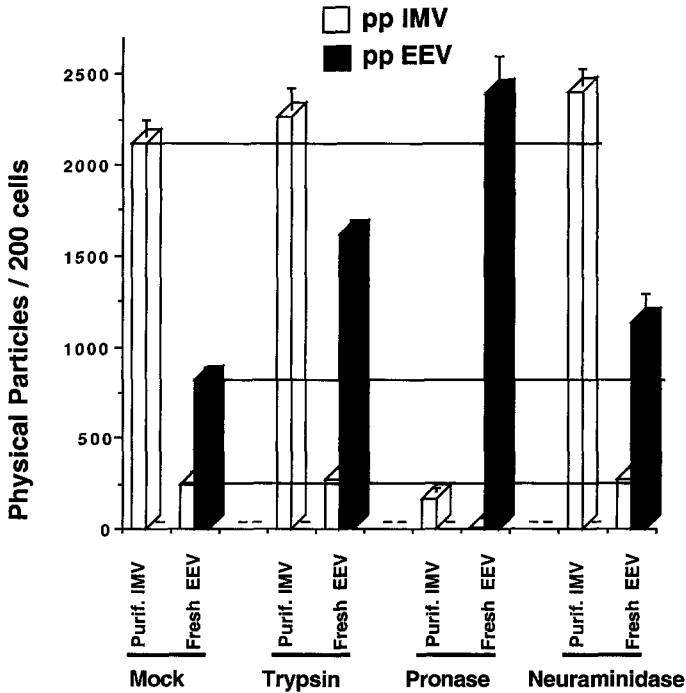


FIG. 4. Cell surface protease treatment affects IMV and EEV binding differently. Mock- or enzyme-treated RK_{13} were cells grown in a 1-well culture chamber slide (Nunc) and were infected on ice for 1 hr (0.5 ml per 1-well chamber slide) with either purified IMV (10 pfu/cell) or fresh EEV (5.2 pfu/cell, 78% of the pfu being resistant to MAb 5B4/2F2 neutralization) diluted in PBS plus 2% FBS. After washing, the cells were treated as described in the text to reveal IMV and EEV virions by double immunofluorescent staining. Numbers of IMV and EEV virions bound on the surface of 200 cells were then determined by confocal microscopy. Data presented are the average \pm SD for triplicate measurements.

interpretation was that the IMV and EEV virions bound to different regions of the same receptor and that by binding to a particular epitope of the receptor, MAb B2 was able to inhibit the binding of only IMV. To exclude the possibility that EEV was able to interact with the MAb B2 reactive receptor despite its capping, we used double immunofluorescent staining to visualize simultaneously MAb B2 reactive molecule clusters and EEV (Fig. 5, color insert). One hundred cells, containing 254 bound EEV, were examined by confocal microscopy to determine the relative localization of EEV-binding sites and MAb B2 reactive molecule clusters.²⁰ All but six EEV particles (which were observed at the periphery of MAb B2 reactive molecule clusters) were present at positions clearly isolated from the MAb B2 clusters, and three representative cells are shown in Fig. 5. This provided definitive data that the receptors used by IMV and EEV are different and

illustrated an important feature of the binding assay: namely it could provide steric information about the binding sites used by a virus in relation to a defined antigen or binding site used by another virus.

Virus Entry Assay Using Confocal Microscopy

The entry of enveloped viruses, like VV, requires the fusion of their envelope with a cellular membrane. The fusion is mediated by viral envelope proteins and can be categorized by the optimal pH required. Viruses that enter the cell in a pH-independent manner (neutral pH) fuse at the plasma membrane or eventually after being internalized within endosomes. In contrast, viruses that enter the cell in a low pH-dependent manner fuse only after internalization and exposure to an acidic environment of an intracellular vesicle.³⁴

The result of the fusion is the release of the structure containing the viral genome and associated proteins into the cytosol of the infected cell. This structure is called the core for VV or capsid for other enveloped viruses. Because confocal microscopy was able to quantify individual particles bound on the cell surface, we considered that it might be possible to adapt this technique to study virus penetration by detecting virus cores inside the cell. To do this we searched for an immunofluorescent staining method that would detect uncoated cores (after virus had entered the cell) but not intact virions (virions still bound onto the cell surface or internalized whole). Suitable results were obtained with an antibody raised against VV cores using the following procedure.

IMV particles were not recognized by this rabbit anticore antiserum if they were untreated or fixed with paraformaldehyde and then permeabilized. It is likely that fixed and permeabilized IMV particles were not stained due to the formation of a lattice around the core by the cross-linking of IMV membrane proteins during fixation. This lattice may prevent access of antibodies to core epitopes despite further permeabilization. However, cores released from IMV after treatment of IMV with Nonidet P-40 (NP-40), or cores present within the cytoplasm were recognized by this antibody.³¹ Samples were therefore first fixed and then permeabilized (as described in Methods) before immunofluorescent staining with a rabbit serum raised against virus cores. The ability of this procedure to detect exclusively intracellular cores resulting from virus entry but not virions adsorbed on the cell surface is illustrated in Fig. 6 (color insert). Purified IMV virions were bound to cells at 4°, and after a short incubation 4 or 37°, cells were fixed, permeabilized, and stained with α -D8L MAb and α -core serum (Fig. 6, color insert). Staining with α -D8L revealed the presence of virions on

³⁴ M. Marsh, *Biochem. J.* **218**, 1 (1984).

the surface of cells that had been incubated at either temperature, although fewer were present after incubation at 37° as many virions had already entered the cell (compare Figs. 6a and 6b). However, α -core serum identified structures only when virus entry was allowed (37°) (compare Figs. 6b and 6e). The merged image (Fig. 6f) demonstrated the core-positive structures did not stain with α -D8L.

Anticore Positive Structures Are Intracellular but Not within Lysosomes

Before using this approach as a way to quantify virus entry, it was necessary to demonstrate that the α -core positive structures were intracellular and did not represent noninfectious virions being degraded within lysosomes.

Optical sections through cells that had been treated to visualize the plasma membrane and virus cores revealed that α -core positive structures were either colocalizing with the plasma membrane or were internal of it (Fig. 7f, color insert). In contrast, staining with α -D8L revealed virions only colocalizing with the plasma membrane (Fig. 7c). To determine if the α -core positive structures colocalizing with the plasma membrane were intracellular or on the cell surface, VV-infected cells were fixed, but not permeabilized, before staining (Figs. 7g–7l). No α -core positive structures were detected without permeabilization (Fig. 7k), indicating that cores were exclusively intracellular.

The possibility that α -core positive structures represented virus being degraded in lysosomes rather than uncoated cores resulting from virus entry was excluded by the simultaneous visualization of lysosomes labeled with Rd-dextran and α -core positive structures. Merged images of lysosomes and cores showed that these were not coincident.³¹

Weak Bases Affect EEV but Not IMV Entry

The penetration assay described in this article provided a simple way to quantify virus entry and to investigate its inhibition by chemicals. The weak bases chloroquine and ammonium chloride affect the entry of viruses that are dependent on a low pH pathway by preventing pH reduction in endosomes and phagosomes.³⁴ The kinetics of IMV and EEV entry in the presence or absence of weak bases was therefore investigated (Fig. 8).

The kinetics of IMV and EEV entry were measured up to only 1 hpi because at later times cores became clustered in the perinuclear region and could not be quantified accurately. Consequently, the total number of virus particles able to enter cells could not be determined. Figure 8 shows that

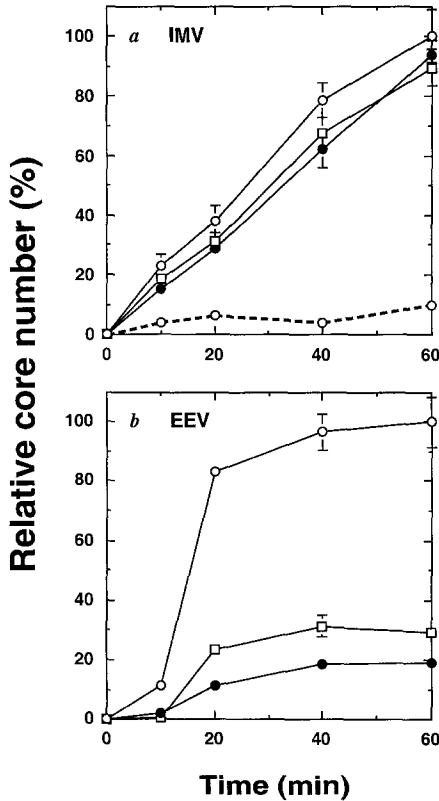


FIG. 8. Effect of weak bases on IMV and EEV entry. Confluent RK₁₃ cells were grown on glass coverslips and preincubated with MEM-2% HFBS (○) or the same containing ammonium chloride (20 mM) (●) or chloroquine (0.1 mM) (□) for 1 hr at 37°. Cells were infected for 1 hr on ice with purified IMV (10 pfu/cell) (a) or fresh EEV (3.5 pfu/cell) (b) diluted in the same preincubation medium. The open circle-dotted line symbol in (a) represents cells that were treated without drugs and infected with IMV containing a neutralizing concentration of MAbs 5B4/2F2. Cells were washed and incubated at 37° with preincubation medium for the indicated time and then washed with cold PBS and treated as described in the text to reveal intracellular cores by indirect immunofluorescent staining. The numbers of cores in 200 cells that were selected randomly were then determined by confocal microscopy. Data are expressed as percentages of the number of cores at time 60 min for the control and are the average \pm SDs for triplicate measurements. At time 60 min, control cells infected with purified IMV and fresh EEV contained a mean of 1482 and 732 cores, respectively.

IMV and EEV enter cells with different kinetics. Whereas the number of cores deriving from IMV entry increased with linear progression and had not plateaued by 1 hpi, the number of cores deriving from EEV entry had plateaued by 20 min and reached 83 and 96% of the level at 1 hpi by 20

and 40 min, respectively (Fig. 8b). The number of cores derived from IMV entry was reduced by 90% by MAb 5B4/2F2, demonstrating that this antibody blocks IMV entry (Fig. 8a).

The weak bases chloroquine or ammonium chloride affected EEV and IMV entry differently: whereas the number of cores deriving from IMV entry was unaltered by these drugs (Fig. 8a), cores resulting from EEV entry were reduced by 71 and 81%, respectively (Fig. 8b, time 60 min). This indicated that EEV but not IMV enters cells by a low pH-dependent pathway.

Discussion

This section describes new methods for the analysis of virus binding to and entry into cells that are based on confocal microscopy. These techniques are illustrated with a study of the binding and entry of VV. The methods have been particularly useful for studying VV because this virus produces two different forms of infectious virion that are antigenically and biologically distinct and are produced in widely differing amounts. Moreover, the EEV form of VV cannot be purified from contaminating IMV without disrupting the integrity of the outer envelope. Such rupture does not destroy virus infectivity because the IMV particle within the outer envelope remains infectious, but a damaged EEV particle with both IMV and EEV antigens exposed might bind to cells via either type of antigen. Purified EEV preparations therefore are unsuitable for binding and entry assays. These problems were overcome by using fresh unpurified virus that contains both EEV and IMV and simultaneously identifying and distinguishing these forms of virus by double immunofluorescent staining followed by confocal microscopy. Data obtained with the methods described in this article have helped to establish that the IMV and EEV virions bind to different cellular receptors and enter cells by different mechanisms.

In addition to the advantages specific to the study of VV due to the two infectious forms of virus, the methods offer several other desirable features. (i) They can use fresh, unpurified virus preparations that are unlabeled. Thus there is no need to use radioactive tracers during the growth of virus or to label the virus after purification with, for instance, fluorescent markers or biotin. Potentially these latter methods might compromise the virion integrity or change its biological properties. (ii) The method generates absolute numbers of virions per cell, not mean numbers representing the average number of virions bound in the whole cell population. Therefore the binding assay could identify specific cells within a mixed cell population that are binding virus particles. For VV, the identification of cells that are unable to bind IMV and EEV, or either form of virus,

would be a useful step toward identifying the cellular receptors for these viruses by expression cloning. (iii) The methods may be used to determine the particle infectivity ratios of viruses and to identify the proportion of virions that bind to cells that give rise to a productive infection. (iv) The methods provide steric information about the site on a cell to which a virion binds in relation to specific cellular antigens or the binding sites for other virions. This was illustrated by the binding of EEV to sites distinct from that identified by a MAb that blocked IMV binding. In addition, the site within cells to which uncoated virus cores or capsids migrate can be studied. (v) In studies of virus entry, the use of antibodies that recognize different virion antigens can identify which antigens are left at the cell surface and the kinetics with which different core or capsid antigens become exposed during uncoating.

In conclusion, we have described novel methods based on confocal microscopy to investigate VV binding and entry. Those methods do not require purified or labeled virus, provide absolute numbers of virus or cores/cell, give steric information concerning the position of the virus or the core, and allow the dissection of the replication cycle by investigating only binding or entry. Although the utility of those techniques has been demonstrated here with VV, they should be applicable to any virus larger than 50 nm.

Acknowledgments

Dr. Alain Vanderplasschen is a permanent senior research assistant of the Fonds National Belge de la Recherche Scientifique at the University of Liège (Belgium). This work was supported by a program grant from the UK Medical Research Council (PG8901790) and an equipment grant from the Wellcome Trust.

[34] Fluorescent Labels, Confocal Microscopy, and Quantitative Image Analysis in Study of Fungal Biology

By RUSSELL N. SPEAR, DANIEL CULLEN, and JOHN H. ANDREWS

Introduction

Microscopy in the study of fungi has been applied basically in two contexts. First, the fungus in isolation can be the subject of investigation, in which case studies typically have focused on cell dynamics, morphogenesis, cytochemistry, and organelle or spore structure and development. Within the past decade, laser scanning confocal microscopy (LSCM) has become